AGU Monograph April 21, 1994

Kinetic Aspects of Reconnection at the Magnetopause

STEPHEN A. FUSELIER

Lockheed Palo Alto Research Laboratory, Palo Alto, California

Observations presented here support the kinetic (or single particle) description of reconnection where ions interacting with the magnetopause conserve their pitch angles or change them by equal amounts as in adiabatic motion. These observations include ion reflection and transmission at the magnetopause and time of flight effects associated with the magnetopause layers, with an emphasis here on ion reflection. Velocities of the reflected distributions predicted from this kinetic description are in good agreement with observed velocities. However, predicted velocities for the transmitted distributions are often higher than observed ones. Reflected distributions are also heated at the magnetopause; however, this heating is less important than the large scale ion motion. Reflection coefficients at the magnetopause are high (averaging 30%), appear to be the same on either side of the magnetopause, and have little or no dependence on ion mass. Time of flight effects result from the finite extent of the reconnection layers and are best observed at the edges of the layers.

INTRODUCTION

Early modelers of the magnetopause suggested that a field free cavity could exist around a stagnation point in the subsolar region when the interplanetary magnetic field (IMF) was nearly radial [e.g., *Beard,* 1964]. It was suggested that solar wind ions convecting along the Earth-sun line could enter this field free region, ballistically reflect off the magnetopause, and return in the sunward direction. This type of reflection at the magnetopause has not been observed. In the current understanding of the magnetopause and magnetosheath, such a field free cavity cannot form even for radial IMF because the field rotates across the bow shock and in the magnetosheath such that a stagnation line rather than a stagnation point is formed [e.g., *Phan et al.,* 1994].

Although the concept of magnetic reconnection was introduced about the same time as these early magnetopause models [*Dungey,* 1961], the possibility of particle reflection (as well as transmission) in association with magnetic reconnection was not considered until the 1980's. The physics of ion reflection was applied to the magnetopause independently by *Cowley* [1980; 1982] and *Sonnerup et al.* [1981]. This application was motivated by the physics of single particle motion in thin current sheets that had already been applied to other regions such as the Earth's magnetotail and the bow shock [e.g., *Sonnerup,* 1969]. In this regard, ion reflection off the magnetopause during reconnection is a manifestation of kinetic (or single particle) processes at the open boundary.

A qualitative sketch of the reflection and transmission process is shown in Figure 1 (from *Gosling et al.* [1990a]). For southward interplanetary magnetic field, reconnection most likely occurs in the subsolar region. Magnetosheath ions convecting in from the left will either reflect off the magnetopause or cross the boundary and enter the magnetosphere. Similarly, both high energy ring current ions and low energy ionospheric ions convecting in from the right will either reflect off the magnetopause or cross the boundary and enter the magnetosheath. The reflected and transmitted ions remain within the separatrices S1 and S2 in Figure 1 and the edges of the electron and ion

layers (E1, I1 and E2, I2) can be offset due to time of flight effects (see *Gosling et al.*, [1990a]). Transmitted magnetosheath ions and reflected magnetospheric ions form the low latitude boundary layer (LLBL) on the magnetospheric side of the magnetopause. Similarly, transmitted magnetospheric and reflected magnetosheath ions form the magnetosheath boundary layer (MSBL) on the magnetosheath side of the magnetopause.

The reflection and transmission process as discussed by *Cowley* [1982] and *Sonnerup et al.* [1981] does not specify whether an ion incident on the magnetopause will reflect or be transmitted. However, it does describe ion motion upon reflection or transmission. After specifying a reflection coefficient at the magnetopause, three primary assumptions are needed to determine the collective motion of reflected and transmitted ions at the magnetopause. The first assumption is the existence of a deHoffman-Teller frame [*deHoffman and Teller*, 1950]. In this frame, the electric field on both sides of the magnetopause is zero. This is a particularly important assumption for the multicomponent plasma at the magnetopause because it requires that all ion distributions on both sides of the magnetopause have the same **E**×**B** drift speed (i.e., that magnetic field gradients are not important). Indeed, **E**×**B** drifts for the individual plasma components in the LLBL and MSBL are nearly the same [e.g., *Gosling et al.*, 1990b; *Fuselier et al.*, 1991; 1993].

The second assumption is that the magnetopause is a time stationary, one-dimensional rotational discontinuity. Under this assumption, the bulk flow velocity of the center of mass of the distribution in the deHoffman-Teller frame is the Alfven speed. This assumption will be discussed later and is also discussed in other articles in this Monograph. Finally, the third assumption is that ions either do not change their pitch angles upon reflection or transmission or change their pitch angles in a constant way as in adiabatic motion. Under this assumption, stochastic processes such as wave particle interactions are less important that the kinematic processes of ion motion in the large scale magnetic and electric fields. A consequence of this assumption is that ions

with the same incident velocity but different mass/charge will have the same velocity upon transmission across the magnetopause. This is indeed the case; transmitted magnetosheath H^+ and He^{2+} bulk flow velocities in the LLBL were found to be nearly the same [*Paschmann et al., 1989*].

With these three primary assumptions, Figure 2 shows cuts through the ion distributions in the MSBL (a) and the LLBL (b) for a magnetopause crossing north of the reconnection site during southward IMF (adapted from *Cowley et al.* [1982] and *Fuselier et al.* [1991]). These cuts are along the magnetic field in the **E**×**B** frame of the plasma. The separation between the incident and reflected distributions is twice the local Alfven velocity ($2V_A$). The velocity changes upon reflection and transmission are related to the energy gain individual ions experience in their interaction with the rotational discontinuity and are discussed in detail elsewhere [e.g., *Sonnerup et al.*, 1981; *Cowley*, 1982; *Paschmann et al.*, 1989]. For a crossing south of the reconnection site, the reflected and transmitted distributions are mirror imaged about zero parallel velocity. Time of flight effects (discussed later) become important as the observation point moves away from the magnetopause. Therefore, it is assumed that the distributions in Figure 2 are measured in the respective boundary layers very near the magnetopause current layer. Also, additional assumptions needed to produce Figure 2 are that the velocities of the inflowing plasma parallel to the magnetic field are small on both sides of the magnetopause and that the incident solar wind H^+ distribution dominates the plasma density on both sides of the magnetopause. These assumptions are valid for the subsolar region [e.g., *Fuselier et al.*, 1993; *Phan et al.*, 1994] and result in the special case where the deHoffman-Teller velocity (V_{dHT} in Figure 2) bisects the incident and reflected ion distributions and the transmitted and reflected distributions have the same velocity (the Alfven velocity) in this frame.

The purpose of this paper is to present and interpret observations of the kinetic aspects of reconnection at the magnetopause. The aspects discussed here are ion reflection and transmission at the magnetopause and time of flight effects, with an emphasis on reflection. Interpretation of these observations will include 1) reflection and transmission as evidence for reconnection 2) the relative importance of heating and other stochastic effects compared to kinematic processes 3) the determination of the deHoffman-Teller frame 4) the relationship between incident and reflected ion distributions 5) time of flight effects on the observed distributions and 6) the difference between ion reflection at the bow shock and at the magnetopause.

OBSERVATIONS

Ion reflection and transmission

Figure 2 shows two features of the magnetopause region that make it difficult to distinguish incident, reflected, and transmitted ion distributions. First, if the component of the deHoffman-Teller velocity parallel to the magnetic field is small compared to the thermal speed of the incident solar wind distributions, then it is difficult to distinguish the incident and reflected magnetosheath components in the MSBL (Figure 2a). In the subsolar region, the several hundred km/s thermal speeds of the incident magnetosheath H^+ and He^{2+} distributions usually limits the observation of reflected ions to cases where the deHoffman-Teller velocity is also a few hundred km/s. For velocities less than this limit, the incident and reflected distributions merge and can be misinterpreted as parallel heating in the MSBL.

A second feature that causes difficulties is the dominance of the transmitted magnetosheath H^+ population in the LLBL. Typical H^+ densities are 10 to 100 times larger than cold magnetospheric ion densities in the LLBL [*Fuselier et al.*, 1993]. This dominance combined with heating of the reflected distribution (discussed below) makes observing

ion reflection in the LLBL very difficult unless ion composition instruments that resolve individual ion species are used.

Despite these difficulties, magnetosheath ion reflection in the MSBL has been observed at low latitudes [*Sonnerup et al.*, 1981; *Gosling et al.*, 1990c; *Fuselier et al.*, 1991] and at high latitudes [*Gosling et al.*, 1991]. Magnetospheric ion reflection in the LLBL has also been observed for the cold low energy component [*Fuselier et al.*, 1991] and the high energy ring current component [*Scholer and Ipavich*, 1983].

An example of ion reflection and transmission in the MSBL is shown in Figure 3. This event from the ISEE-1 data was the first reported evidence of solar wind proton reflection and low energy magnetospheric ion transmission in the MSBL [*Sonnerup et al.*, 1981]. For this crossing in the subsolar region, the stress balance test indicated that the magnetopause was approximately consistent with a one-dimensional rotational discontinuity although the predicted velocity change across the magnetopause was somewhat higher than the observed one [*Sonnerup et al.*, 1981]. Figure 3 shows solar wind He^{2+} and magnetospheric He^{+} distributions measured by the plasma composition experiment on ISEE-1. The B_{zGSE} component of the magnetic field (from the ISEE-1 magnetometer) is shown in the lower left hand corner. The spacecraft was in the magnetosphere/LLBL at 0040 UT and in the magnetosheath at 0100 UT. Magnetic field rotations at 0044, 0046, and 0051 UT are magnetopause crossings. Short bars indicate where the He^{2+} and He^{+} distributions were measured. The upper panels show contours of constant phase space density (two contours per decade of phase space) in 2-dimensional velocity space. The measurement plane is nearly centered on the ecliptic with the V_x direction toward the sun and the V_y direction toward dusk. The magnetic field direction is shown by the arrow and is approximately in the field of view of the instrument.

The distribution in the left hand panel in Figure 3 was measured in the magnetosheath well after the final outbound magnetopause crossing. It is a typical anisotropic magnetosheath He^{2+} distribution with very low bulk flow velocity both toward the magne-

topause (in the $-V_x$ direction) and perpendicular to the magnetopause (in the $\pm V_y$ direction). The two distributions in the middle panel were measured in the MSBL near the magnetic field rotation (i.e., the magnetopause current layer). The distribution near zero velocity is the incident magnetosheath distribution and the one displaced along the magnetic field is the reflected magnetosheath distribution. The cut parallel to the magnetic field below this panel shows that the incident and reflected distributions are separated by $2V_A$, as predicted in Figure 2. The reflected distribution is heated and contains approximately 6% of the total He^{2+} density. The heating is seen as a wider spacing of the contours of the reflected distribution when compared to the incident magnetosheath distribution. Comparing the incident magnetosheath distributions in the left and middle panels, there is little evidence of heating of this distribution in the MSBL.

The He^{+} distribution in the right hand panel of Figure 3 was also measured in the MSBL near the magnetopause. This is the transmitted cold magnetospheric He^{+} distribution (Figure 2a) (first noted by *Sonnerup et al.* [1981] for this event). The magnetospheric distribution was originally near zero drift velocity in the LLBL but, upon crossing the magnetopause, gained significant energy so that it had a bulk flow velocity along the magnetic field that was somewhat smaller than, but comparable to that of the reflected He^{2+} distribution in the middle panel.

An example of ion reflection and transmission in the LLBL is shown in Figure 4. The event in Figure 4 is from the AMPTE/Charge Composition Explorer data and has not been reported previously. Low energy magnetospheric He^{+} and magnetosheath He^{2+} measured by the hot plasma composition experiment (HPCE) on the CCE spacecraft are shown in a format similar to that in Figure 3. The B_z component of the magnetic field in the lower left hand panel (from the CCE magnetometer experiment) shows that the spacecraft was in the magnetosheath at 0015 UT ($B_z<0$) and in the magnetosphere at 0030 UT ($B_z>0$). The single magnetopause crossings for this event (also in the subsolar region) was at 0020 UT.

Short bars show where the He^+ and He^{2+} distributions were measured. The top panels show contours of constant phase space density similar to those in Figure 3. The measurement plane of the AMPTE instrument was tilted nearly 90° from that of the ISEE-1 instrument in Figure 3. Thus, the distributions in Figure 4 are in a plane approximately tangent to the subsolar magnetopause viewed from the sun with the V_z direction approximately perpendicular to the ecliptic plane and the V_y direction approximately in the ecliptic plane toward dusk.

The distribution in the left hand panel was measured in the magnetosphere well away from the LLBL. It is a low energy, highly anisotropic He^+ distribution often found in the outer magnetosphere [e.g., *Fuselier et al.*, 1991; *Anderson and Fuselier,* 1994] and it is convecting very slowly toward the magnetopause (~10 km/s in the V_z direction). The He^+ distributions in the middle panel were measured in the LLBL very near the magnetopause current layer. The same incident magnetospheric distribution in the left hand panel has picked up a substantial perpendicular flow velocity in the V_y direction in the LLBL. The magnetic field direction in the middle panel, drawn through the perpendicular component of the transmitted magnetosheath H^+ (and He^{2+}) distribution (the bulk of the plasma in the LLBL) indicates that the incident He^+ distribution picked up the **E**×**B** drift of the transmitted magnetosheath plasma in the LLBL. In addition to the incident He^+ distribution in the LLBL, the middle panel shows a second, hotter distribution displaced in the antiparallel direction at approximately twice the Alfven velocity. This is the reflected He^+ distribution predicted in Figure 2. The direction of the reflected distribution in Figure 4 is opposite the one in Figure 2 because the CCE spacecraft crossed the magnetopause south and not north of the reconnection line. The reflected distribution is hotter than the incident one and contains almost 36% of the total He^+ density in the LLBL.

The LLBL He^{2+} distribution in the right hand panel was measured simultaneously with the He^+ distribution in the middle panel. In addition to the transmitted magnetosheath

He^{2+} distribution at -260 km/s antiparallel to the magnetic field (open circle), there is some low energy magnetospheric He^{2+} at near zero parallel velocity that, like its He^{+} counterpart, acquired the **E**×**B** drift of the transmitted magnetosheath population. The transmitted magnetosheath He^{2+} was initially at near zero drift velocity in the magnetosheath but, upon crossing the magnetopause, gained significant energy.

The deHoffman-Teller velocity for the event in Figure 4 bisects the incident and reflected He^{+} distributions in the LLBL so that these distributions are at nearly $\pm V_A$ along the magnetic field (see Figure 2). In this frame, the transmitted magnetosheath distribution should be flowing along the magnetic field (in this case in the anti-parallel direction) at the local Alfven velocity. The right hand panel of Figure 4 shows that the He^{2+} bulk velocity is somewhat lower than V_A in the deHoffman-Teller frame. This is also true for the transmitted H^{+} distribution (not shown) since its velocity is approximately the same as that of the transmitted He^{2+}.

Table 1 contains density and temperature ratios of reflected ion distributions reported to date. The 1984 events are from a study of magnetopause crossings from the AMPTE/CCE spacecraft [Fuselier et al., 1993]. The density and temperature ratios were determined from moments of the incident and reflected distributions in the MSBL and LLBL. Transmission and reflection on both sides of the magnetopause was discussed in detail by *Fuselier et al.* [1991] for one of these events (18 October 1984). The 1978 events are from the ISEE-1 and -2 data sets. The He^{2+} observations from the 8 September 1978 event are in Figure 2 and the H^{+} density and temperature ratios for this event were determined from (unpublished) distribution functions from the Los Alamos/Garching Fast Plasma Experiment (M. F. Thomsen, personal communication). The other density and temperature ratios were determined by fitting two temperature maxwellian functions to published incident and reflected distributions.

Considering individual species (columns), Table 1 shows that ions reflect off the magnetopause in large numbers with reflection coefficients averaging about 30%. Reflected distributions are also about a factor of three hotter than the incident distributions, indicating heating either in the reflection process or after the distributions have reflected (through wave-particle interactions). Although common data for several species are sparse, an intercomparison of columns in Table 3 and their averages shows that reflection coefficients do not vary significantly with species nor are they very different from one side of the magnetopause to the other. All ion species on both sides of the magnetopause appear to respond similarly to the magnetopause current layer.

Time of Flight Effects

As discussed above, time of flight effects have been ignored in the predictions in Figure 2. These effects can be safely ignored so long as observations (such as those in Figures 3 and 4) are made sufficiently close to the magnetopause current layer. Time of flight effects are the direct result of the finite extent of the reconnection region. For example, when the reconnection site is below an observing spacecraft, ions enter the LLBL all along the magnetopause from near the observation point to the magnetic field X line. Plasma convection toward the magnetopause in the LLBL creates a low speed cutoff parallel to the magnetic field in the transmitted distribution because 1) the lower the parallel velocity of the ion, the further south from the observation point the ion crossed the magnetopause and 2) ions cannot come from further away than the magnetic field X line.

For observation points near the magnetopause and for reasonably high deHoffman-Teller velocities, the low speed cutoff due to time of flight effects is below the deHoffman-Teller velocity and therefore does not affect the observed distributions. However,

as the observation point moves closer to the boundary between the LLBL and the magnetosphere, the low speed cutoff velocity increases and can become considerably higher than the deHoffman-Teller velocity. In fact, at the separatrix (S2 in Figure 1), the low speed cutoff is at infinite velocity.

Time of flight effects are best seen near this earthward edge of the LLBL by comparing ion and electron distributions in the layer. The extremely high cutoff velocities near the earthward edge of the LLBL and the fact that transmitted magnetosheath electrons have much higher velocities than transmitted ions leads to a layer within the LLBL that contains magnetosheath electrons and no magnetosheath ions. This layer is between I2 and E2 in Figure 1. An excellent example of this layer is described in detail by *Gosling et al.* [1990a]. There should also be a similar layer of transmitted magnetospheric electrons and no transmitted ions in the MSBL (between I1 and E1 in Figure 1).

DISCUSSION

Observations presented in Figures 3 and 4 and in Table 1 show that reflection (and transmission) of ions occurs at the Earth's magnetopause. These observations are strong evidence in support of the kinetic picture of reconnection at the magnetopause where individual ions either preserve their pitch angle or change it a through adiabatic motion in the interaction with the open boundary. Although these observations provide strong evidence for reconnection, they would be difficult to use in a statistical survey of reconnection at the magnetopause. The observations are limited to fairly high deHoffman-Teller drift speeds in the MSBL and require mass resolving detectors (as well as reasonably high deHoffman-Teller drift speeds) in the LLBL. At lower speeds (near the thermal speed of the incident distributions), it is difficult to distinguish incident and reflected distributions.

Another feature of the magnetopause region that makes observations of ion reflection difficult is heating of the reflected ion distribution. Table 1 shows that this heating

can be substantial, at least in the perpendicular direction. Parallel heating is more difficult to quantify but does occur (compare the incident and reflected He^+ distributions in Figure 4). Heating may be the result of scattering of the ions in the current layer (so that near adiabatic motion is violated) or the result of pitch angle scattering of the reflected distribution by waves.

Although the heating is substantial, it does not dominate the kinematic motion of the ions in the large scale electric and magnetic fields. This kinematic motion is determined by the change in the ion velocity in the deHoffman-Teller frame of reference. Reflected and transmitted ion distributions provide a relatively way to determine the deHoffman-Teller frame [*Fuselier et al.*, 1991]. In the events presented here near the subsolar magnetopause, the deHoffman-Teller frame velocity is simply the velocity that bisects the incident and reflected distributions in the MSBL in Figure 3 and in the LLBL in Figure 4. In this frame, the incident and reflected distributions are at $\pm V_A$, the local Alfven velocity. These velocities are consistent with predictions of ion interaction with a time stationary, one-dimensional rotational discontinuity.

Although predicted and observed velocities for the incident and reflected distributions are nearly in agreement, predicted and observed velocities for the transmitted ion distributions show less agreement. Often, the transmitted distributions on both sides of the magnetopause (Figures 3 and 4) are observed to have velocities less than the predicted Alfven velocity in the deHoffman-Teller frame. Since the transmitted protons dominate the mass density in the LLBL [*Fuselier et al.*, 1993], lower velocities of the transmitted magnetosheath component will translate into bulk (or fluid) velocities across the magnetopause than that are lower than those predicted by stress balance across a time stationary, one-dimensional rotational discontinuity. The observed bulk flow velocities in the LLBL do average lower than those predicted from stress balance [e.g., *Paschmann et al.*, 1986]. Thus, the fluid treatment (that predicts the velocity

through the stress balance test) and the kinetic treatment (that predicts the transmitted and reflected velocities through single particle motion) both fail to predict the observed velocities of the transmitted ions at the magnetopause. The differences between the observed and predicted velocities in the fluid treatments are typically not large (~25%) [e.g., *Paschmann et al.*, 1986] and such good agreement is really extraordinary.

The differences between observed and predicted velocities may indicate that the magnetopause is not a simple one dimensional discontinuity [e.g., *Fuselier et al.*, 1993]. This suggestion is supported by the fact that the separation between the incident and reflected distributions is both observed and predicted to be $2V_A$ (see Figures 3 and 4) because the reflection process takes place along essentially the same field line as the incident distribution. Transmitted ion distributions in Figures 3 and 4 are probably not as simply connected along the same single field line from their origin on one side of the magnetopause to the point of observation on the other.

Time of flight effects in the LLBL also support the suggestion that transmitted distributions are not simply connected along the same field line from the MSBL to the LLBL. The finite travel time between the observation point in the LLBL and the entry point where a particle crosses the magnetopause is best exemplified in the separate ion and electron layers in the LLBL illustrated schematically in Figure 1 (see *Gosling et al.* [1990a]). The much higher speed of the electrons entering the LLBL allow them to be observed closer to the separatrix that separates magnetospheric field lines from those magnetospheric field lines that have reconnected at the magnetopause. These time of flight effects are not accounted for in the predictions in Figure 2.

Although ion reflection and transmission at the magnetopause and time of flight effects have been observed and several aspects appear to be reasonably well understood, there are other important features of these kinetic processes that are not understood and are open to further research. One feature that is not understood is the amount of

reflected ions at the magnetopause. As pointed out in the introduction, the predictions for magnetopause reflection deal with the ion motion upon reflection and do not predict a reflection coefficient. A larger sample of ion reflection and a better understanding of the reflection process itself may allow such a prediction. Along this same line, part of the original motivation for suggesting that ion reflection may occur at the magnetopause was the success in applying this process to the bow shock. It is interesting to compare the results of ion reflection at the two boundaries because, although the physical process is the same, the results are vastly different. The bow shock reflection process [*Sonnerup,* 1969] produces H^+ ion beams almost uniformly at about 1% of the incident solar wind H^+ density and these beams containing almost no solar wind He^{2+} [e.g., *Fuselier and Thomsen,* 1992]. In contrast, reflection at the magnetopause produces beams that average ~30% of the total density and all ion species reflect with nearly equal probability (Table 1). An adequate explanation of these differences may be include consideration of the very different incident flow speed to thermal speed ratios (very large for the bow shock and very small for the magnetopause) and differences between ion interaction with a supercritical shock and a rotational discontinuity. Finally, some other areas open for research include reflected ions as a source of free energy for waves in the boundary layers and the variation of the deHoffman-Teller velocity, the Alfven velocity, and the low speed cutoff velocity (due to time of flight effects) as the observation point moves from the magnetopause to the edge of the boundary layer.

Acknowledgments. The author gratefully acknowledges discussions with B. U. Ö. Sonnerup and J. T. Gosling. The ISEE Fast Plasma Experiment data for 8 Sept 1978 were provided by M. F. Thomsen. The ISEE magnetometer data were provided by C. T. Russell through the NSSDC. The CCE magnetometer data were provided by T. A. Potemra through the Applied Physics Laboratory Science Data Center. Research at Lockheed was funded by NASA through

contract NAS5-30565 and the NASA Guest Investigator program through contract NAS5-31213.

REFERENCES

Anderson, B. J., and S. A. Fuselier, Response of thermal ions to electromagnetic ion cyclotron waves, *J. Geophys. Res.*, in press, 1994.

Beard, D. B., The effect of an interplanetary magnetic field on the solar wind, *J. Geophys. Res.*, *69*, 1159, 1964.

Cowley, S. W. H., Plasma populations in a simple open model magnetosphere, *Space Sci. Rev.*, *26*, 217, 1980.

Cowley, S. W. H., The causes of convection in the Earth's magnetosphere: A review of developments during the IMS, *Rev. Geophys.*, *20*, 531-565, 1982.

deHoffman, F., and E. Teller, Magnetohydrodynamic shocks, *Phys. Rev.*, *80*, 692, 1950.

Dungey, J. W., Interplanetary field and the auroral zones, *Phys. Rev. Lett.*, *6*, 47-48, 1961.

Fuselier, S. A., and M. F. Thomsen, He^{2+} in field-aligned beams: ISEE results, *Geophys. Res. Lett.*, *19*, 437, 1992.

Fuselier, S. A., D. M. Klumpar, and E. G. Shelley, Ion reflection and transmission during reconnection at the Earth's subsolar magnetopause, *Geophys. Res. Lett.*, *18*, 139-142, 1991.

Fuselier, S. A., D. M. Klumpar, and E. G. Shelley, Mass density and pressure changes across the dayside magnetopause, *J. Geophys. Res.*, *98*, 3935, 1993.

Gosling, J. T., M. F. Thomsen, S. J. Bame, T. G. Onsager, and C. T. Russell, The electron edge of the low latitude boundary layer during accelerated flow events, *Geophys. Res. Lett.*, *17*, 1833, 1990a.

Gosling, J. T., M. F. Thomsen, S. J. Bame, R. C. Elphic, and C. T. Russell, Cold ion beams in the low-latitude boundary layer during accelerated flow events, *Geophys. Res. Lett., 17,* 2245, 1990b.

Gosling, J. T., M. F. Thomsen, S. J. Bame, R. C. Elphic, and C. T. Russell, Plasma flow reversals at the dayside magnetopause and the origin of asymmetric polar cap convection, *J. Geophys. Res., 95,* 8093, 1990c.

Gosling, J. T., M. F. Thomsen, S. J. Bame, R. C. Elphic, and C. T. Russell, Observation of reconnection of interplanetary and lobe magnetic field lines at the high-latitude magnetopause, *J. Geophys. Res., 96,* 14,097, 1991.

Paschmann, G., I. Papamastorakis, W. Baumjohann, N. Sckopke, C. W. carlson, B. U. Ö Sonnerup, and H. Lühr, The magnetopause for large magnetic shear: AMPTE/IRM observations, *J. Geophys. Res., 91,* 11,099, 1986.

Paschmann, G., S. A. Fuselier, and D. M. Klumpar, High speed flows of H^+ and He^{++} ions at the magnetopause, *Geophys. Res. Lett., 16,* 567-570, 1989.

Phan, T.-D., G. Paschmann, W. Baumjohann, N. Sckopke, and H. Lühr, The magnetosheath region adjacent to the dayside magnetopause: AMPTE/IRM observations, *J. Geophys. Res., 99,* 121, 1994.

Scholer, M., and F. M. Ipavich, Interaction of ring current ions with the magnetopause, *J. Geophys. Res., 88,* 6937, 1983.

Sonnerup, B. U. Ö., Acceleration of particles reflected at a shock front, *J. Geophys. Res., 74,* 1301, 1969.

Sonnerup, B. U. Ö., G. Paschmann, I. Papamastorakis, N. Sckopke, G. Haerendel, S. J. Bame, J. R. Asbridge, J. T. Gosling, and C. T. Russell, Evidence for magnetic field reconnection at the Earth's magnetopause, *J. Geophys. Res., 86,* 10,049-10,067, 1981.

TABLE 1. Density and Perpendicular Temperature Ratios of Reflected Ions at the Magnetopause

		Magnetosheath Reflection H^+		Magnetosheath Reflection He^{2+}		Magnetospheric Reflection He^+	
Date	MP Time	n_r/n_{tot}%	$T_{r\perp}/T_{s\perp}$	n_r/n_{tot}%	$T_{r\perp}/T_{s\perp}$	n_r/n_{tot}%	$T_{r\perp}/T_{s\perp}$
11 Jun 78	2247[1]	30	5.8	-	-	-	-
12 Aug 78	1835[2]	4	3.1	-	-	-	-
8 Sep 78	0043[3]	9	2.6	6	1.9	-	-
7 Oct 84	0020	16	2.5	23	2.6	36	6.2
18 Oct 84	1302[4]	37	1.2	50	6.2	30	1.7
18 Oct 84	1648	56	1.9	55	2.8	-	-
19 Oct 84	0810	15	2.8	17	2.6	-	-
Average		27 ± 18	2.8 ± 1.6	30 ± 21	3.2 ± 1.7	~33	~3.9

[1]Gosling et al. [1991].

[2]Gosling et al. [1990] "FTE".

[3]Sonnerup et al. [1981] estimated 20% reflected H^+ in the MSBL. Scholer and Ipavich [1983] estimated 10-50% reflected ring current H^+ in the LLBL for this magnetopause crossing.

[4]Fuselier et al. [1991].

Fig. 1. Qualitative sketch of the magnetopause region for quasi-stationary reconnection (from *Gosling et al.* [1990a]). Magnetosheath (magnetospheric) ions convecting in from the left (right) either reflect off the magnetopause and enter the MSBL (LLBL) or cross the magnetopause and enter the LLBL (MSBL).

Fig. 2. Qualitative sketch of the ion distributions expected in the MSBL (a) and the LLBL (b) for a magnetopause crossing north of the reconnection line. If V_{dHT} is small and the magnetosheath temperature is large, the incident and reflected magnetosheath distributions in the MSBL will not be easily distinguished. Also, the transmitted magnetosheath distribution dominates the plasma in the LLBL, making it difficult to observe the reflected cold magnetospheric distribution.

Fig. 3. An example of ion reflection and transmission in the MSBL. The upper panels show contours of constant phase space density in two-dimensional velocity space and the lower panels show B_z and parallel cuts through two distributions. Distribution functions in the upper panels were measured in the MSBL and magnetosheath, where $B_z<0$. The distribution at near zero velocity in the first two panels is the incident magnetosheath He^{2+} distribution. The second distribution in the middle panel at $2V_A$ along the magnetic field is the reflected magnetosheath distribution. Concurrent with this reflected distribution is the transmitted He^{+} distribution in the third panel.

Fig. 4. An example of ion reflection and transmission in the LLBL. The format is similar to Figure 3. The incident cold (few eV) magnetospheric distribution (left hand panel) picks up the $\mathbf{E}\times\mathbf{B}$ drift speed of the transmitted magnetosheath He^{2+} in the LLBL (middle panel). The second distribution in the middle panel at about $2V_A$ along the magnetic field is the reflected He^{+} distribution. The transmitted He^{2+} distribution is shown in the left hand panel.

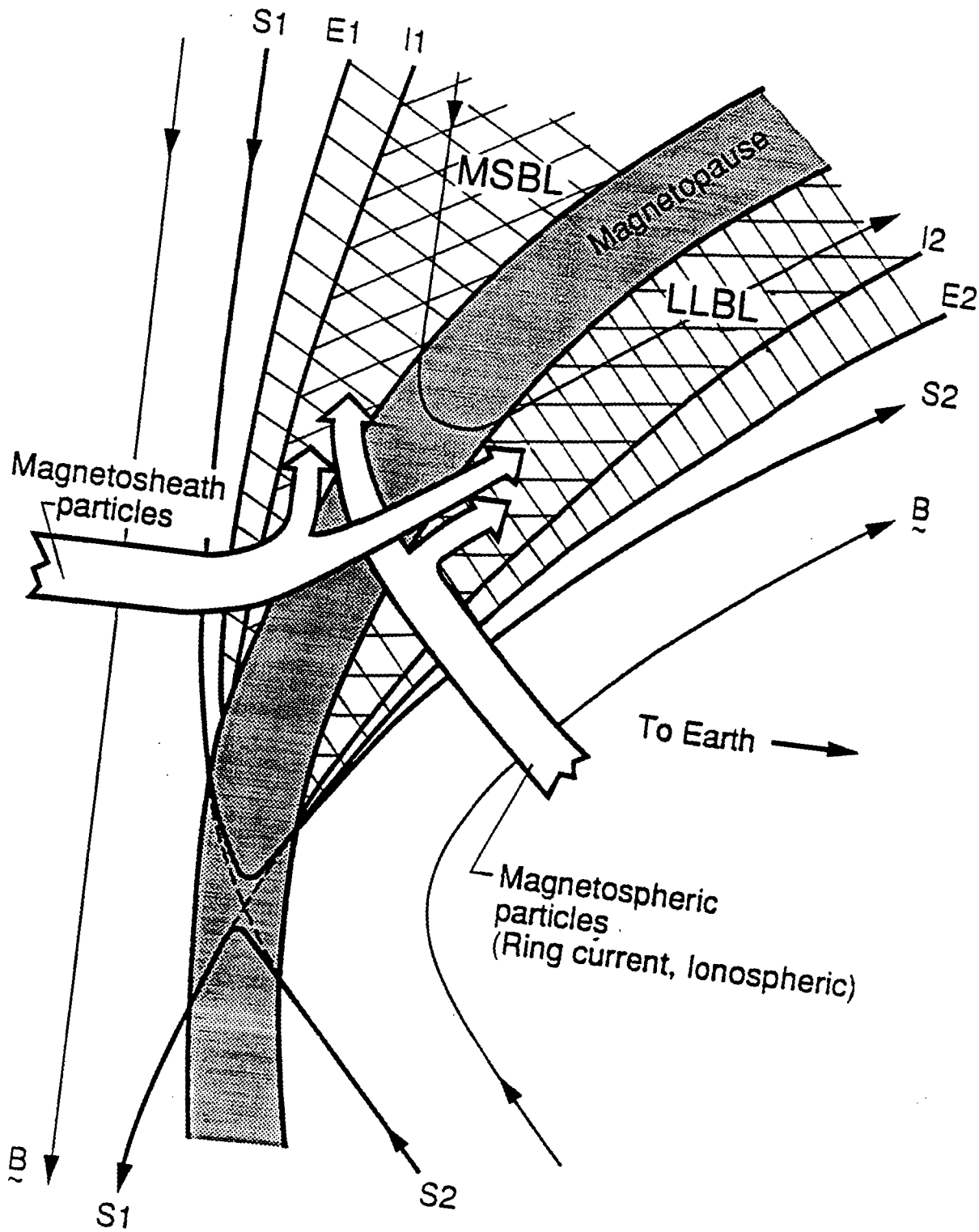
S1
E1
I1
MSBL
Magnetopause
I2
LLBL
E2
S2
Magnetosheath
particles
B
To Earth
Magnetospheric
particles
(Ring current, Ionospheric)
B
S1
S2

Figure 1

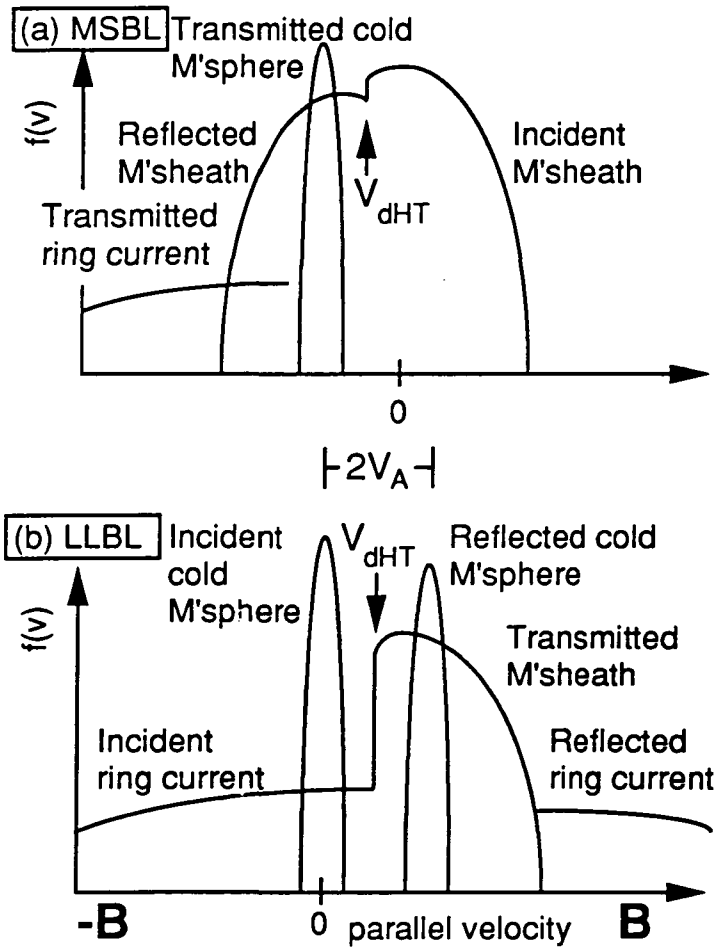
(a) MSBL
Transmitted cold
M'sphere
f(v)
Reflected
M'sheath
Incident
M'sheath
V_{dHT}
Transmitted
ring current
0
$2V_A$
(b) LLBL
Incident
cold
M'sphere
V_{dHT}
Reflected cold
M'sphere
f(v)
Transmitted
M'sheath
Incident
ring current
Reflected
ring current
-B
0
parallel velocity
B

Figure 2

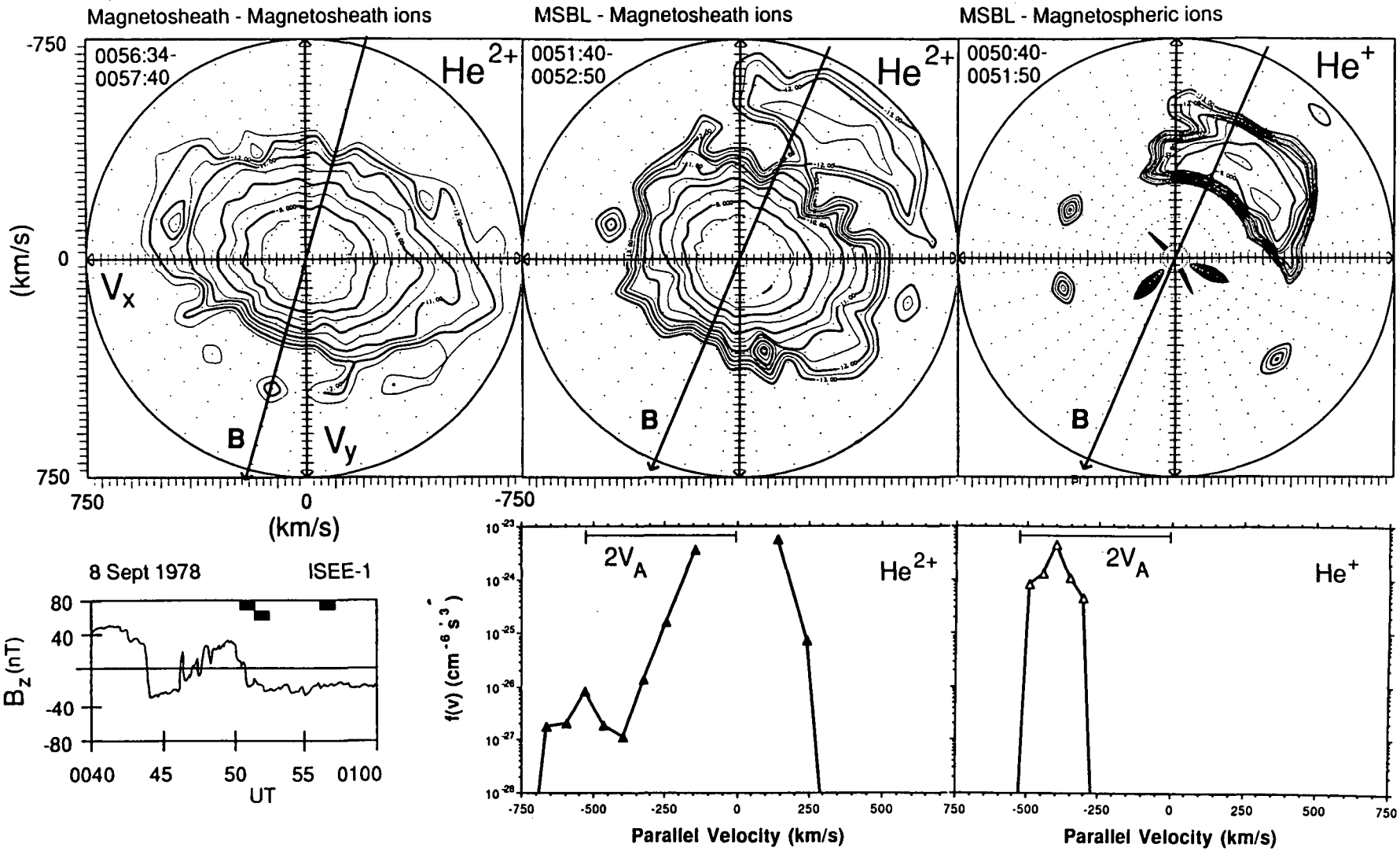
Magnetosheath - Magnetosheath ions
MSBL - Magnetosheath ions
MSBL - Magnetospheric ions
0056:34-
0057:40
0051:40-
0052:50
0050:40-
0051:50
He2+
He2+
He+
-750
0
750
(km/s)
Vx
Vy
B
B
B
750
0
-750
(km/s)
8 Sept 1978
ISEE-1
80
40
-40
-80
Bz (nT)
0040
45
50
55
0100
UT
2VA
2VA
He2+
He+
f(v) (cm-6 s3)
10-23
10-24
10-25
10-26
10-27
10-28
-750
-500
-250
0
250
500
750
Parallel Velocity (km/s)
Parallel Velocity (km/s)

Figure 3

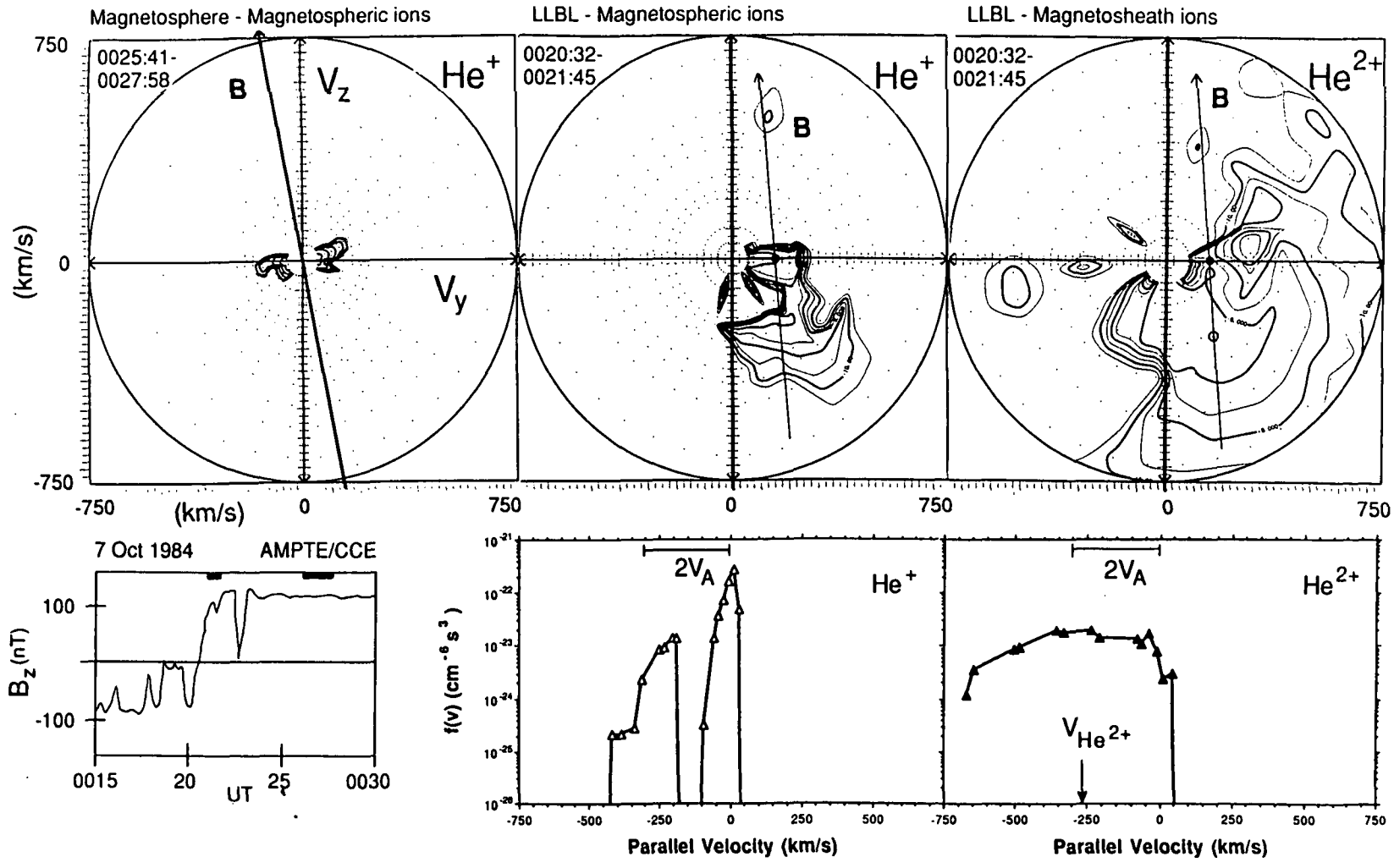
Magnetosphere - Magnetospheric ions
LLBL - Magnetospheric ions
LLBL - Magnetosheath ions
0025:41-
0027:58
0020:32-
0021:45
0020:32-
0021:45
B
V_z
V_y
He^+
He^{2+}
750
0
-750
(km/s)
7 Oct 1984
AMPTE/CCE
B_z(nT)
100
-100
0015
20
25
0030
UT
$2V_A$
$V_{He^{2+}}$
f(v) (cm^{-6} s^3)
Parallel Velocity (km/s)

Figure 4